Restricted Relaxation in Polymer Nanocomposites near the Glass Transition

Hongbin Lu and Steven Nutt*

MCGF Composites Center, Department of Materials Science, University of Southern California, Los Angeles, California 90089

Received January 15, 2003

ABSTRACT: The relaxation behavior of organically modified layered silicate−epoxy nanocomposites was studied using a combination of standard and temperature-modulated differential scanning calorimetry. For such nanocomposites, the silicate layers were intercalated in the matrix resin and epoxy networks were grafted onto the silicate layer surfaces. Enthalpy recovery that occurred during physical aging was used as a probe to detect restricted relaxation behavior in the nanocomposites. Addition of the intercalated nanoparticles resulted in a slower overall relaxation rate and a wider distribution of relaxation times. The nanocomposites also showed a higher glass transition temperature compared to that of the unreinforced resin. To explain the observed results, a domain relaxation model was proposed that included three possible relaxation modes. On the basis of this model, the restricted relaxation arising from intercalated and exfoliated layered silicates can be understood.

Introduction

The unique properties of polymer nanocomposites inspire continued efforts to develop a variety of novel materials and devices.[1−3] In addition, these materials provide opportunities to better understand certain fundamental aspects of polymer science.[4,5] For example, the design and optimization of properties of nanocomposite systems relies heavily on the molecular dynamics of polymers. In such systems, two distinct types of dynamic behavior have been reported in the literature. When the polymer molecules are intercalated between two parallel solid surfaces separated by 1.5−2.0 nm, a segmental dynamic mode is observed that is much faster than that of bulk polymers, as reported by Anastasiadis[6] and by Vaia.[7] Such fast dynamics of polymers confined within clay galleries is similar to the relaxation behavior of small molecules confined within nanopores, for which the calorimetric glass transition temperature T_g decreases with decreasing pore size.[8−11] In contrast, a slower relaxation mode in intercalated or exfoliated clay−polymer hybrid systems has been observed by Messersmith[12] and Kanapitsas,[13] using dynamic mechanical analysis and broadband dielectric relaxation spectroscopy. In addition, Lee[14] and Li[15] showed that in polyhedral oligosilsesquioxane (POSS) reinforced polymer nanocomposites the nanosized cage structures that were incorporated into polymer chains effectively hindered the relaxation of polymers, causing the T_g to increase with increasing concentration of the cage structures. Apparently, the understanding of restricted relaxation behavior in polymer nanocomposites is incomplete and requires further exploration and investigation.

The restricted relaxation behavior has attracted considerable attention since Jackson and McKenna[8a] first reported a calorimetric study of the vitrification of glass forming liquids in controlled pore glasses. Various experimental techniques such as thermal analysis,[7,8,16] dielectric relaxation,[6,17] ellipsometry,[18] X-ray reflectivity,[18d,19] Brillouin light scattering[18e,20] and molecular dynamics simulation[21] have been utilized to explore the molecular mechanism involved under confined conditions. Meanwhile, the effects of various confining environments on the molecular dynamics of glass formers have been investigated. These environments include thin polymer surface films on substrates,[22] amorphous polymers confined between crystalline lamellae,[23] cross-linking polymer networks,[24] molecular liquids impregnated in porous materials, and nanocomposites. Despite these efforts, experimental observations concerning the restricted dynamics are contradictory, and the relevant theoretical depictions have not yet been well established.

Because of the characteristic long-chain molecules, polymers are sensitive to the local environment, and the relaxation dynamics near T_g is essentially cooperative.[25−28] When a polymer is cooled through the glass transition region, the physical properties of the polymer in the nonequilibrium state (at temperature lower than T_g), such as volume and enthalpy, gradually recover to new equilibrium values through the configurational rearrangement of polymer segments. The rate of the rearrangement or relaxation process depends on the local environment surrounding the relaxation entities and hence reflects the extent of environmental restriction on those entities. In this paper, we use the change in calorimetric enthalpy that occurs during physical aging (i.e., enthalpy relaxation) as a probe to study the restricting effect of nanoparticles on the relaxation dynamics of polymers near the glass transition. The remarkable retardation dynamics that derive from the restriction effect of nanoparticles is analyzed. Also, we tentatively propose a domain relaxation model to explain the experimental phenomena observed here and by other investigators and attempt to establish a general understanding of the characteristic relaxation behavior that occurs in intercalated and exfoliated MMT−polymer nanocomposites.

* To whom correspondence should be addressed: e-mail nutt@usc.edu.

10.1021/ma034049b CCC: $25.00
Published on Web 05/07/2003

Table 1. Characteristic Parameters for Epoxy Nanocomposites

		epoxy nanocomposites (DGEBA−DDS−MMT)			
	neat resin	3 phr[a]	5 phr	7 phr	10 phr
d_{001}, Å		54.3	56.0	48.5	45.7
T_g, °C	190.34	194.87	195.59	196.3	196.78

[a] phr is the abbreviation for per hundred resin.

Experimental Section

The polymer nanocomposites synthesized in this work consisted of organically modified layered silicates and an epoxy resin matrix. The layered silicates were supplied by Southern Clay Products with the trade name Cloisite 30B, hereafter abbreviated as MMT (montmorillonite). The epoxy resin selected was diglycidyl ether of bisphenol A (DGEBA) from Shell Chemical's Epon 828, cured by stoichiometric 4,4′-diaminodiphenyl sulfone (DDS) with different solid contents. To synthesize the nanocomposites, a select amount of dry MMT powder was first mixed with DGEBA at 90 °C, and the mixture was degassed under vacuum. Subsequently, DDS was added to the mixture and mixed for 20 min at 150 °C. The resulting mixture of DGEBA, DDS, and MMT was precured for 2 h at 160 °C and postcured for 2 h at 240 °C and 1 h at 260 °C. No exothermic peak was observed in the cured specimens between room temperature and 300 °C. The resulting epoxy networks are believed to directly attach to the surfaces of the MMT silicate layers by a cross-linking reaction between the epoxide and the hydroxyl groups of the alkylammonium ions located on the layer surfaces of MMT.[12] The silicates are dispersed in the polymer such that the silicate is intercalated in the polymer. The basal spacings for all the epoxy nanocomposites, measured by X-ray diffraction, are given in Table 1.

The variation in calorimetric enthalpy reflecting the relaxation behavior of the different epoxy−MMT nanocomposites was measured using standard differential scanning calorimetry (DSC 2920, TA Instruments, Inc.). Annealing experiments for all specimens were conducted at $T_g - 20$ °C. The enthalpies recovered after different annealing times were measured by heating from 30 to 250 °C at a constant rate of 10 °C/min. The effect of cooling rate on the enthalpy relaxation of nanocomposites was observed at 0.5, 0.7, 1.0, 3.0 and 5.0 °C/min, respectively. To determine the distribution of relaxation times for the different hybrid systems, changes in complex heat capacity near the glass transition were monitored for all specimens using temperature-modulated differential scanning calorimetry (MDSC). The parameters for the MDSC experiments were as follows: average cooling rate, 0.5 °C/min; temperature amplitude, 0.5 K; modulated period, 60 s.

Results and Discussion

Representative DSC spectra for the neat resin and for the nanocomposites with different MMT contents are presented in Figure 1. The T_g's for all specimens were determined from the midpoints of the corresponding glass transition regions. The measured T_g values are plotted as a function of MMT content in the left inset of Figure 1 and are also listed in Table 1. The widths of the glass transitions, ΔT, as determined by the method shown in Figure 1, are given for all specimens as a function of MMT content in the right inset of Figure 1. The increasing MMT content results in a shift of T_g to higher temperatures, and the glass transition regions become broader relative to the neat resin.

The T_g determined for the neat resin subjected to the curing procedure described earlier is 190.3 °C, which is higher than the 175 °C stated by the supplier[29] but lower than the 212 °C reported by LeMay and Kelley.[30] The former (low) T_g is obtained when the system contains a small amount of the curing promoter BF_3−monoethylamine (about 1 wt %) and is cured for 5 h at 125 °C, followed by a postcure for 1 h at 200 °C. The plasticizing effect of small molecules (curing promoter) slightly reduces the T_g of the resulting resin, as pointed out by the manufacturer. The latter (high) T_g is realized when the system is cured for 15 h at 200 °C without any additives. Such a long cure time favors the completion of the slow-cure reaction at this temperature and minimizes possible decomposition reactions. However, the procedure inevitably results in a higher packing density of polymer chains, which tends to increase the T_g of the resin. Our neat resin and MMT nanocomposites obtained via the current curing procedure exhibit no exothermic peak(s) in the temperature range from 30 to 300 °C. Furthermore, thermogravimetric analyses under conditions identical to the present cure procedure provide no evidence of thermal decomposition. This indicates that the T_g values determined herein for all the samples are valid. The fact that T_g increases with MMT content derives from the effect of MMT on the segmental mobility of epoxy networks.

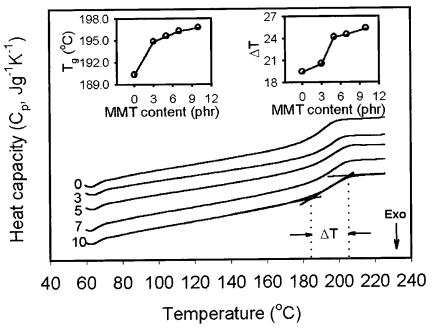

Figure 1. DSC curves for the neat resin and the hybrids obtained at a heating rate of 10 °C/min after erasing the previous thermal history. The left inset gives the variation of T_g obtained from these curves with MMT content, and the right inset gives the width of glass transition region for all the specimens.

The effect of MMT on the T_g of epoxy resins reported in the literature is somewhat controversial. On one hand, a decrease in T_g for epoxy−MMT systems has been reported. Zilg and Mulhaupt et al.[31] explored the effect of various amine modifiers on the T_g of stoichiometric epoxy/anhydride hybrid systems and concluded that effective intercalation significantly reduced the T_g of the resulting composites. Chen and Ober[32] and Shi and Pinnavaia[33] attributed the reduction of T_g to the formation of an interphase, in which surfactant molecules attached to the silicate surface effectively plasticize the intergallery polymer. On the other hand, an increase in the T_g of epoxy−MMT nanocomposites has also been noted by several researchers. When studying the effect of MMT on the final properties of DGEBA/benzyldimethylamine nanocomposites, Messersmith and Giannelis[12] found that 4 vol % of MMT increased the mechanical loss peak temperature of the nanocomposite by 4 °C compared with the neat resin. The increase in T_g was attributed to chemical bonding in the interphase between the silicate and epoxy matrix, which reduced the mobility of polymer segments near the solid surface. In addition, other authors found that MMT had no significant effect on the T_g of epoxy nanocomposites, while some reports indicated that the effect might be minimized by means of optimizing the fabrication procedure of nanocomposites.[34,35] The experimental observations cited above underscore the complexity of factors that can affect the T_g of epoxy nanocomposites.

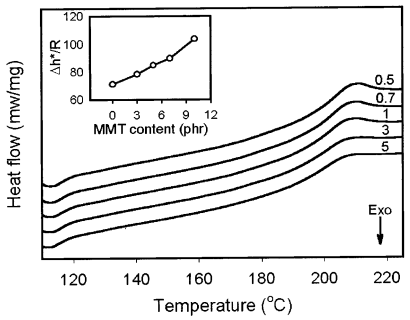

Figure 2. DSC curves for the nanocomposites of 5 phr MMT obtained at heating a rate of 10 °C/min after cooling at the rate of 0.5, 0.7, 1.0, 3.0, and 5.0 °C/min. The inset shows the activation energy of segmental relaxation changing with MMT content.

An improved understanding of the relaxation behavior of polymer nanocomposites during the glass transition requires further study.

Physical aging (or enthalpy relaxation) experiments under selected conditions were conducted to determine the restriction effects of MMT on the segmental motion in epoxy nanocomposites. Figure 2 shows the representative DSC curves for nanocomposite specimens (5 phr MMT) after cooling at various rates. A typical overshoot effect can be observed as cooling rate decreases. However, the magnitude of the overshoot effect (at the same cooling rate) differed among the nanocomposite samples. With increasing MMT content, the overshoot effect becomes weaker (not shown here). This implies that there may be some structural difference among these samples, which can be generally characterized in terms of a limiting fictive temperature, T_f', as described by Ritland[36] and Moynihan.[37] The T_f' can be obtained directly from the original heating DSC curves by means of an "equal area" method[37] and is closely related to the cooling rate, q, by

$$\mathrm{d}\ln|q|/\mathrm{d}(1/T_f') = -\Delta h^*/R \qquad (1)$$

where Δh^* is the activation energy of the relaxation time controlling the structural relaxation and R is the universal gas constant. Equation 1 allows us to directly observe the effect of MMT on the temperature dependence of segmental relaxation time of epoxy networks. The Δh^* values obtained from eq 1 are presented for all samples in the inset of Figure 2. Clearly, the addition of MMT results in an increase in Δh^*.

The activation energy Δh^* has been linked to the configurational energy barrier and reportedly reflects the cooperative nature of a relaxation process.[38] In addition, the dependence of Δh^* on the chain flexibility of polymers has been reported.[39] On studying the enthalpy relaxation of semicrystalline polyimides, it was found that Δh^* increased with decreasing size of the flexible linkage.[39] Thermodynamically, this is reasonable because the higher chain rigidity naturally requires a higher configurational activation threshold. For a thermosetting epoxy resin, however, the impact of cross-link density on Δh^* may be of greater importance. The increase in Δh^* with increasing cross-link density of the epoxy network indicates that the increasing cross-link point number increases restriction during segmental relaxation. To some extent, this is similar to the current epoxy nanocomposite systems. An increase in the MMT content creates more segments anchored/attached on the surface of silicate layers (see below),

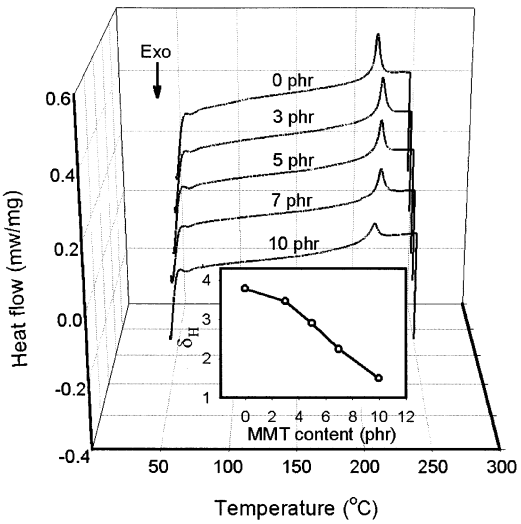

Figure 3. DSC curves for the samples with different MMT contents obtained at a heating rate of 10 °C/min after annealing for 372 h at $T_g - 20$ °C. The inset shows the corresponding recovery enthalpy changing with MMT content.

and the network structure formed thereby has to surmount a higher energy barrier to reach the activated state and to accomplish the corresponding configurational rearrangement.

The overshoot effect observed after nonisothermal aging can be more clearly observed from isothermal annealing experiments. The effect originates primarily from the enthalpy recovered during annealing or slow cooling (sometimes called "enthalpy loss"), reflecting the segmental relaxation behavior of polymers during the glass transition. Figure 3 shows the original DSC curves for samples after isothermal annealing at $T_g - 20$ °C. The effect of MMT on the segmental relaxation of epoxy networks can be clearly observed. For instance, the recovered enthalpy δ_H for the neat resin after aging 372 h at $T_g - 20$ °C is 3.78 J g^{-1}, whereas the recovered enthalpy corresponding to the nanocomposites with 10 phr MMT is 1.50 J g^{-1}. Under the same annealing condition, the decrease in δ_H with increasing MMT content is also presented in the inset of Figure 3. The δ_H values were obtained from the area difference between the annealed curve and the unannealed reference curve of the same sample.

The recovery enthalpy during physical aging depends on the thermal history that a glass experiences and on related experimental variables, such as cooling rate, annealing temperature, annealing time, and heating rate. When these variables are fixed, as here, the smaller recovery enthalpy of nanocomposites can be ascribed to the slower relaxation rate of epoxy segments arising from MMT restriction. This retardation may result in a shift in T_g toward higher temperature, as shown in Figure 1.

Isothermal enthalpy relaxation experiments provide a direct measure of the overall relaxation rate of polymer segments. For instance, for a bulk sample, the relaxation rate β_H is usually defined as

$$\beta_H = \mathrm{d}\delta_H/\mathrm{d}(\log t_a) \qquad (2)$$

where t_a refers to the isothermal aging time.[40] However, for the confined systems studied here, defining the relaxation rate this way may be problematic. In recent work, Simon and McKenna et al.[41] analyzed the relax-

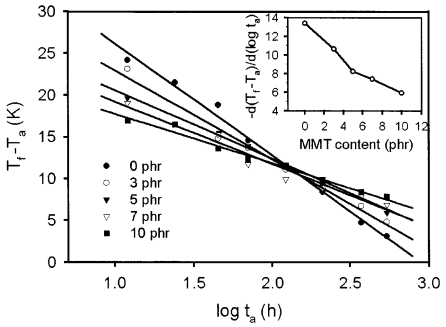

Figure 4. Semilogarithmic plot of ($T_f - T_a$) vs aging time (log t_a). The inset gives the slope of the lines obtained by linear fitting the semilogarithmic experimental data, i.e., the overall relaxation rate of epoxy networks changing with MMT content.

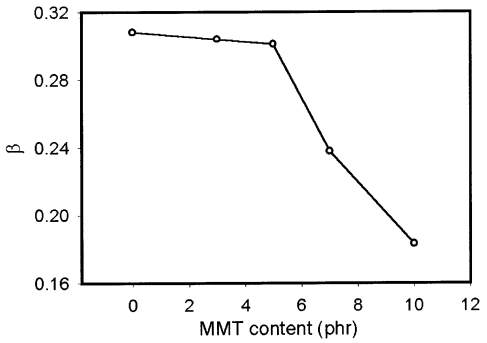

Figure 5. Nonexponentiality parameter β changes with MMT content, reflecting the distribution of relaxation times.

ation behavior of *o*-terphenyl confined in controlled pore glasses with different pore diameters. They found that the confined molecules might relax to equilibrium states different from the corresponding bulk material, which could result in the incorrect use of eq 2 in confined systems. When a system is annealed at some temperature T_a, it will approach the corresponding equilibrium state. Thus, the difference between the fictive temperature corresponding to some annealing time and T_a reflects the extent to which the system has approached equilibrium. Accordingly, we can define a new overall relaxation rate R_E, as

$$R_E = -\mathrm{d}(T_f - T_a)/\mathrm{d}(\log t_a) \qquad (3)$$

From eq 3, the linear relationships between ($T_f - T_a$) and log(t_a) for all the samples are found and shown in Figure 4. The slopes of these lines give the overall relaxation rate of each sample, R_E. The R_E values are plotted as a function of MMT content in the inset of Figure 4. The reduction in R_E with increasing MMT content is consistent with the variation in T_g and Δh^* and represents an additional manifestation of the restriction effect of MMT on the segmental relaxation near the glass transition.

Such restriction effects can be associated with a broader distribution of relaxation time, because, as shown in Figure 1, we have seen a wider glass transition region for the present composite systems. According to published reports, the cooperative configurational rearrangement of supercooled polymer glasses is not a Debye process and cannot be depicted with a single relaxation time.[26,27] Usually, a stretched exponential function (Kohlrausch−Williams−Watts equation) is used to approximate the time dependence of the segmental relaxation function, given by

$$\phi(t) = \exp[-(t/\tau)^{\beta}] \qquad (4)$$

where τ is the KWW relaxation time and β is the phenomenological shape parameter (also called the nonexponentiality parameter, $0 < \beta < 1$) characterizing the distribution of relaxation time. A smaller β value implies a broader distribution of relaxation time, while a larger β value represents a narrower distribution. Various factors affect the distribution of relaxation time of epoxy resins, including increased cross-link length,[42] incomplete cure reaction,[43] nonstoichiometric ratio between epoxy and curing agent,[44] and the presence of a reactive diluent.[45] All of these factors have been found to narrow the distribution of relaxation time or increase the β value. However, none of the cited reports have examined the effect of MMT particles on the distribution of relaxation time during the glass transition of epoxy resins.

The two approaches normally used to obtain the nonexponentiality parameter β in enthalpy relaxation experiments are curve-fitting[46] and peak-shift methods.[47] Recently, another method based on the MDSC technique was proposed by Hutchinson[48] and Montserrat.[49] This method involves measurement of the complex heat capacity of glasses, C_p^*, as a function of temperature during the glass transition. The corresponding β value is determined from the normalized inflectional slope of C_p^*, i.e., $\bar{S} = (\mathrm{d}C_p^*/\mathrm{d}T)/\Delta C_p^*$ (for details, see refs 48 and 49). The β values measured by this method for the neat epoxy resin and nanocomposites are shown in Figure 5. Incorporation of MMT broadens the distribution of relaxation time of epoxy segments, and the extent of broadening increases with MMT content. This result is in agreement with the observed expansion of the glass transition region.

To summarize, the experimental results for the epoxy nanocomposites reveal slower segmental relaxation dynamics, a higher glass transition temperature, slower overall relaxation rate, and a broader distribution of relaxation times compared with the neat epoxy resin. The retarded relaxation observed here differs from the fast dynamics reported by other investigators for nanocomposites with similar intercalated structure.[6,7] To explain the more rapid dynamics, authors have proposed an isolation effect of silicate layers or micropores that diminishes the cooperativity between molecules. This contention has been supported by positron-annihilation-lifetime spectroscopy[50] and NMR experiments.[51] However, these arguments cannot fully account for the slow dynamic behavior exhibited in the present work.

The slow dynamics observed herein can be attributed to the restricted chain mobility in the interfacial layer, in which polymer chains are effectively anchored or attached to the silicate surface. The curing agent DDS can reportedly catalyze both the homopolymerization of DGEBA and the reaction between hydroxyl groups of the alkylammonium ions and the oxirane rings of DGEBA.[52] A possible mechanism involving the base-catalyzed oxirane ring-opening reaction between hydroxyl groups of organically modified MMT and DGEBA was proposed recently by Messersmith and Giannelis.[12] The MMT−glycidyl ether of bisphenol A oligomer formed during the reaction can continue to react with DGEBA, resulting in an epoxy network directly anchored on the silicate layers. These anchored polymer chains form an interphase region where the segment relaxation is slower than in the bulk.

The restriction effect arising from the solid surface has been observed in small-molecule glass-formers. In studies of glass transition behavior of *o*-terphenyl and *o*-terphenyl/polystyrene solution confined in nanopores, Park and McKenna[53] found two glass transitions in DSC thermograms. One of them appeared at a temperature greater than the T_g of the bulk, while the other occurred below the bulk T_g. The former was attributed to a transition of an interacting layer at the pore surface and the latter to a transition of a "core" liquid in the center surrounded by an interacting layer. The distinct relaxation behavior reported is consistent with results obtained via dielectric relaxation[11,17b,24b] and optical Kerr effect spectroscopies.[54]

A similar effect on glass transition might also be observed on the DSC thermograms from the current nanocomposites, assuming a restriction effect arising from the layered silicate surfaces. However, multiple glass transitions were not detected at temperatures different from the bulk T_g in our DSC experiments, aside from the shift of the glass transition to a higher temperature with increasing MMT content. One possible reason is that interfacial layers comprised of polymer segments anchored on silicate surfaces may not exhibit a glass transition within the measured range.[17c] A second possibility is that, in some cases, the contribution of interfacial layers to the segmental relaxation may simply cause an overall shift in T_g to a temperature different from the bulk value. In fact, Forrest et al.[20c] studied confinement effects on the cooperative dynamics of free-standing polymer films and reported that one does not always observe two distinct T_g's and that simulations in fact predict a single T_g for films possessing strong dynamic heterogeneities. Therefore, it is reasonable to assert that the slow dynamics observed here derive largely from the anchored interfacial layers.

The restriction effect of solid surfaces on the segmental relaxation of polymers can be observed more directly from the dynamic study of thin polymer films supported on a substrate. To elucidate the mechanism underlying the anomalous glass transition of supported polymer films, considerable work has been performed since the pioneering work of Keddie, Jones, and Cory.[18b,c] Today, it is well recognized that the restriction effect of solid surfaces can accelerate or hinder the segmental relaxation of polymer molecules, depending on the strength of the polymer−substrate interactions.[55] The dynamic Monte Carlo simulation performed by Bashnagel and Binder[21a] indicated that competition between packing constraints in the bulk and the loss of configurational entropy at the solid interface led to greater monomer and end-monomer density at the solid interface and finally gave rise to reduction in T_g in supported films. On the other hand, molecular dynamic simulations of Torres, Nealey, and de Pablo[21b] clearly revealed that the reduced mobility of the polymer chains due to attractive interactions at the interface caused an elevation in T_g in supported films. The results obtained by simulation are consonant with experimental results reported in the literature.[55]

The physical dimensions of an interfacial layer existing between a polymer and a solid surface have been measured by Litvinov et al.[56] Using an NMR relaxation method that is particularly sensitive to the heterogeneous mobility of polymer chains at solid surfaces, they observed two distinct characteristic decay times for a poly(dimethylsiloxane) (PDMS) layer grafted onto a silica surface. A short decay time corresponded to low-mobility chain portions adjacent to the silica surface, while a longer decay time corresponded to mobile chain segments outside the interface. Assuming complete coverage of the silica surface and a grafted layer of uniform thickness, they estimated that the average thickness of the interphase was 0.7−1.1 nm. This thickness is comparable to the minimum size of the cooperative rearrangement region (CRR) of 1.5−2.0 nm at T_g.[57]

Regardless of the reported contradictions in experiments and simulations, the results cited above clearly indicate that the interfacial layer plays a significant role in the slow dynamics observed in supported films or polymer-grafted solid surfaces. This supports our assertion that the anomalous relaxation behavior observed in the present systems originates primarily from the restriction effect of MMT particles. Nevertheless, one should also note that, for segments intercalated within the gallery of MMT, the effect of interlayer spatial constraint is also an important factor and should not be overlooked. Polymer segments outside the interphase but intercalated within intragalleries of MMT particles may experience an isolation effect if the interlayer spacing is larger than twice the interphase thickness. When polymer molecules are confined within the silicate galleries with a height on the order of 1 nm, the shape of the CRR is significantly perturbed.[6] Such molecules experience less confinement from neighboring molecules and segments because of the isolating effect of the silicate layers, and thus the segmental relaxation may be noncooperative.[6,7]

Recent simulations have shown that the intercalated polymer chains are arranged in discrete subnanometer layers parallel to the crystalline silicate layers,[58] resulting in a dynamic anisotropy with enhanced parallel and reduced perpendicular monomeric mobilities.[59] Such dynamical heterogeneity for nonpolar polymer chains confined within the silicate galleries has been detected by Zax et al. using a combination of ^{2}H NMR spectroscopy and a cross-polarization intensity measurement.[51] They found that the dynamically slowest polymer moieties were in the immediate vicinity of the silicate surface, whereas a faster relaxation mode was characteristic of chain segments located toward the center of the intercalated film, where the local density was lower. For the present end-anchored epoxy segments, the relaxation next to the silicate surface is expected to experience greater constraint relative to the intercalated nonpolar polymer chains and hence exhibit slower relaxation dynamics. Furthermore, the relaxation rate of chain segments outside the interphase should be slower than nonpolar chains midway between the two silicate layers. Thus, local relaxation rates are expected to vary with distance from the silicate surface.

Model Development. From our analysis of the experimental results, we propose a coarse-grained domain relaxation model, as described in Figure 6. In this model, we neglect details of the polymer chains in the interphase and in the central area of the intergallery of silicates. Three relaxation domains are delineated in accordance with the different relaxation rates. The slowest relaxation characteristic (domain I) corresponds to motion of segments located in the interphase, which includes the internal and external surfaces of silicate layers. The fastest mode (domain II) corresponds to the relaxation of segments located in the central area of intergallery of silicates. Here, the retardation from the neighboring segments is shielded by the individual

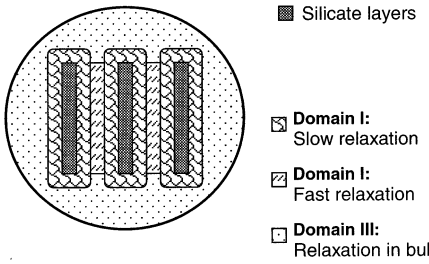

Figure 6. Coarse-grained domain relaxation model depicting the restricted relaxation of the intercalated or exfoliated layered silicate−polymer nanocomposites.

silicate layers. The third relaxation mode (domain III) corresponds to the normal segmental motion of epoxy networks. No retardation and shielding effects are anticipated in this mode.

The proposed domain relaxation model provides a general understanding of the restricted relaxation that occurs in layered silicate−polymer nanocomposites. This phenomenon depends on the extent to which the layered silicates are exfoliated. Fast relaxation dynamics occurs only in intercalated systems. As the extent of exfoliation increases, more polymer chains diffuse into the silicate intergalleries, resulting in greater cooperativity between intercalated segments. Thus, as the gallery spacing increases, the fast relaxation process is diminished. For the case of complete exfoliation, the fast relaxation mode is eliminated, as observed in thin polymer films grafted onto solid substrates.[60] Second, the extent to which segmental relaxation is restricted depends on the strength of interaction between silicate layers and polymer matrices. For polymer chains grafted onto a solid surface, the largest restriction effect is expected, while a much smaller effect is expected for weak interactions between a solid surface and a polymer molecule, such as hydrogen bonding or physical adsorption. Grafting density also plays an important role for the restricted relaxation of interfacial layers. Higher graft density forces the polymer chains in the interfacial layer to be arranged in a high degree of quasi-nematic order with the chains extended nearly to their full lengths. This inevitably leads to a larger restriction effect. In contrast, for nonpolar polymer chains exhibiting weak interactions with silicate surfaces, faster relaxation dynamics is expected compared to polar or grafted polymer chains intercalated within the intergallery of silicates.

The overall relaxation behavior of polymer nanocomposites also depends on the ratio of restricted and unrestricted segmental numbers. This is supported by the remarkable dependence on solid content, as shown in Figure 4. The relaxation dependence on one hand determines the broadness of relaxation time distribution. On the other hand, higher solid contents will result in a percolated network of nanoparticles that can influence relaxation on a different scale. The percolation effect is usually considered to be effective for relaxation of longer time scales, such as the terminal relaxation observed in some rheological measurements. However, recent dynamic mechanical experiments for composite solids seem to indicate that restriction effects do in fact result from the formation of a percolation network.[61] Nevertheless, reports regarding the restriction effects of percolated networks on the segmental relaxation are not fully conclusive, and the issue awaits more detailed and systematic study.

Conclusion

We have studied the restricted relaxation behavior of layered silicate−epoxy nanocomposites using a combination of standard and temperature-modulated DSC. Three typical features were observed, including higher T_g, slower overall relaxation rate, and broader distribution of relaxation times relative to the neat epoxy resin. To explain these experimental results, we have proposed a domain relaxation model that includes three possible relaxation modes. On the basis of this model and analysis of our data, we concluded that the restricted relaxation behavior for intercalated and exfoliated silicate−polymer nanocomposites depended primarily on the extent of exfoliation of the layered silicates and the strength of interaction between the silicate surface and the polymer molecules. Thus, a system with fully exfoliated silicate dispersion and strong interactions (e.g., polymer segments grafted onto silicate surfaces) is expected to exhibit slow relaxation behavior, while a system with intercalated silicates and weak interaction (e.g., nonpolar polymer chains intercalated to the silicate intergallery) should display fast relaxation dynamics. In addition, the overall relaxation behavior of nanocomposites depends on the ratio of restricted and unrestricted segment numbers and thus exhibits a strong dependence on solid content.

The present work has established a physical picture for the molecular motions involved in polymer nanocomposites that contributes to our understanding of the structure−properties relationship. For polymer nanocomposites with layered silicates, a fully exfoliated structure often requires practical synthesis procedures that are specific to the system. In most cases, intercalated structures can be obtained, and these result in relaxation behavior in different time scales. The domain relaxation model presented here can be used to provide a suitable mathematical description for the specific relaxation behavior. The overall relaxation function can be written as a combination of the KWW expressions with different time scales, e.g., $\phi(t) = \phi(t/\tau_1) + \phi(t/\tau_2)\phi(t/\tau_3)$, where τ_1 is the fast relaxation time and τ_2 and τ_3 are the restricted and bulk relaxation times, respectively. The mathematical model is similar to the cooperative relaxation expression suggested by Feldman[62] and is expected to give a better description for the specific relaxation behavior occurring in intercalated nanocomposites than the KWW model with a single relaxation time. In addition, some aspects, especially regarding the percolation effect on relaxation in nanocomposites systems, require further investigation. These are currently being pursued.

Acknowledgment. Support from the TRW Foundation and from the Merwyn C. Gill Foundation is gratefully acknowledged. The authors also express thanks to Prof. Gregory B. McKenna for his valuable suggestions to this manuscript. H. Lu also thanks Mr. Hongbin Shen for assistance with DSC experiments and discussion.

References and Notes

(1) Pinnavaia, T. J.; Beall, G. W. *Polymer-Clay Nanocomposites*; John Wiley & Sons: New York, 2000.
(2) Komarneni, S.; Parker, J. C.; Wollenberger, H. J. *Nanophase and Nanocomposite Materials II*: Symposium, Boston, 1996; Materials Research Society: Pittsburgh, PA, 1997.
(3) Godovsky, D. Y. *Adv. Polym. Sci.* **2000**, *153*, 163.
(4) Giannelis, E. P.; Krishnamoorti, R.; Manias, E. *Adv. Polym. Sci.* **1999**, *138*, 107.

(5) Krishnamoorti, R.; Vaia, R. A. *Polymer Nanocomposites: Synthesis, Characterization, and Modeling*; Oxford University Press: New York, 2002.
(6) Anastasiadis, S. H.; Karatasos, K.; Vlachos, G. *Phys. Rev. Lett.* **2000**, *84*, 915.
(7) Vaia, R. A.; Sauer, B. B.; Tse, O. K.; Giannelis, E. P. *J. Polym. Sci., Polym. Phys.* **1997**, *35*, 59.
(8) (a) Jackson, C. L.; McKenna, G. B. *J. Non-Cryst. Solids* **1991**, *131*−*133*, 221. (b) Jackson, C. L.; McKenna, G. B. *Chem. Mater.* **1996**, *8*, 2128.
(9) Zhang, J.; Liu, G.; Jonas, J. *J. Phys. Chem.* **1992**, *96*, 3478.
(10) Kremer, F.; Huwe, A.; Arndt, M.; Behrens, P.; Schwieger, W. *J. Phys.: Condens. Matter* **1999**, *11*, A175.
(11) Arndt, M.; Stannarius, R.; Groothues, H.; Hempel, E.; Kremer, F. *Phys. Rev. Lett.* **1997**, *79*, 2077.
(12) Messersmith, P. B.; Giannelis, E. P. *Chem. Mater.* **1994**, *6*, 1719.
(13) Kanapitsas, A.; Pissis, P.; Kotsilkova, R. *J. Non-Cryst. Solids* **2002**, *305*, 204.
(14) Lee, A.; Lichtenhan, J. D. *Macromolecules* **1998**, *31*, 4970.
(15) Li, G. Z.; Wang, L.; Toghiani, H.; Daulton, T. L.; Pittman, C. U., Jr. *Polymer* **2002**, *43*, 4167.
(16) (a) Schonhoff, M.; Larsson, A.; Welzel, P. B.; Kuckling, D. *J. Phys. Chem. B* **2002**, *106*, 7800. (b) Schonhals, A.; Goering, H.; Schick, C. *J. Non-Cryst. Solids* **2002**, *305*, 140.
(17) (a) Melnichenko, Y. B.; Schuller, J.; Richert, R.; Ewen, B.; Loong, C. K. *J. Chem. Phys.* **1995**, *103*, 2016. (b) Arndt, M.; Stannarius, R.; Gorbatschow, W.; Kremer, F. *Phys. Rev. E* **1996**, *54*, 5377. (c) Fukao, K.; Miyamoto, Y. *Phys. Rev. E* **2000**, *61*, 1743. (d) Bergman, R.; Swenson, J. *Nature (London)* **2000**, *403*, 283.
(18) (a) Beaucage, G.; Composto, R.; Stein, R. S. *J. Polym. Sci., Polym. Phys.* **1993**, *31*, 319. (b) Keddie, J. L.; Jones, R. A. L.; Cory, R. A. *Europhys. Lett.* **1994**, *27*, 59. (c) Keddie, J. L.; Jones, R. A. L.; Cory, R. A. *Faraday Discuss.* **1994**, *98*, 219. (d) Wallace, W. E.; van Zanten, J. H.; Wu, W. L. *Phys. Rev. E* **1995**, *52*, R3329. (e) Forrest, J. A.; Dalnoki-Veress, K.; Dutcher, J. R. *Phys. Rev. E* **1997**, *56*, 5705.
(19) (a) Orts, W. J.; van Zanten, J. H.; Wu, W. L.; Satija, S. K. *Phys. Rev. Lett.* **1993**, *71*, 867. (b) van Zanten, J. H.; Wallace, W. W.; Wu, W. L. *Phys. Rev. E* **1996**, *53*, R2053. (c) Tsui, O. K. C.; Russell, T. P.; Hawker, C. J. *Macromolecules* **2001**, *34*, 5535.
(20) (a) Forrest, J. A.; Dalnoki-Veress, K.; Stevens, J. R.; Dutcher, J. R. *Phys. Rev. Lett.* **1996**, *77*, 2002. (b) Forrest, J. A.; Dalnoki-Veress, K.; Dutcher, J. R. *Phys. Rev. E* **1998**, *58*, 6109. (c) Forrest, J. A.; Mattsson, J. *Phys. Rev. E* **2000**, *61*, R53.
(21) (a) Baschnagel, J.; Binder, K. *Macromolecules* **1995**, *28*, 6808. (b) Torres, J. A.; Nealey, P. F.; de Pablo, J. J. *Phys. Rev. Lett.* **2000**, *85*, 3221. (c) Lee, J. Y.; Baljon, A. R. C.; Loring, R. F.; Panagiotopoulos, A. Z. *J. Chem. Phys.* **1998**, *109*, 10321. (d) Salaniwal, S.; Kumar, S. K.; Douglas, J. F. *Phys. Rev. Lett.* **2002**, *89*, 258301. (e) Kuppa, V.; Manias, E. *J. Chem. Phys.* **2003**, *118*, 3421.
(22) (a) Forrest, J. A.; Jones, R. A. L. In *Polymer Surfaces, Interfaces and Thin Films*; Karim, A., Kumar, S., Eds.; World Scientific: Singapore, 2000. (b) Forrest, J. A.; Dalnoki-Veress, K. *Adv. Colloid Interface Sci.* **2001**, *94*, 167.
(23) (a) Zhu, L.; Cheng, S. Z. D.; Calhoun, B. H.; Ge, Q.; Quirk, R. P.; Thomas, E. L.; Hsiao, B. S.; Yeh, F. J.; Lotz, B. *J. Am. Chem. Soc.* **2000**, *122*, 5957. (b) Nogales, K.; Ezquerra, T. A.; Batallan, F.; Frick, B.; Lopez-Cabarcos, E.; Balta-Calleja, F. J. *Macromolecules* **1999**, *32*, 2301. (c) Dobbertin, J.; Hannemann, J.; Schick, C.; Potter, M.; Dehne, H. *J. Chem. Phys.* **1998**, *108*, 9062. (d) Zhao, J.; Wang, J.; Li, C.; Fan, Q. *Macromolecules* **2002**, *35*, 3097. (e) Zhukov, S.; Geppert, S.; Stuhn, B.; Staneva, R.; Ivanova, R.; Gronski, W. *Macromolecules* **2002**, *35*, 8521.
(24) (a) Jackson, C. L.; McKenna, G. B. *Rubber Chem. Technol.* **1991**, *64*, 760. (b) Barut, G.; Pissis, P.; Pelster, R.; Nimtz, G. *Phys. Rev. Lett.* **1998**, *80*, 3543.
(25) (a) Angell, C. A. *Science* **1995**, *267*, 1924. (b) Angell, C. A.; Ngai, K. L.; McKenna, G. B.; McMillan, P. F.; Martin, S. W. *J. Appl. Phys.* **2000**, *88*, 3113.
(26) (a) Hodge, I. M. *Science* **1995**, *267*, 1945. (b) Hodge, I. M. *J. Non-Cryst. Solids* **1994**, *169*, 211.
(27) Hutchinson, J. M. *Prog. Polym. Sci.* **1995**, *20*, 703.
(28) Donth, E. *Relaxation and Thermodynamics in Polymers Glass Transition*; John Wiley & Sons: New York, 1993.
(29) General literature from Resolution Performance Products Co..
(30) LeMay, J. D.; Kelly, F. N. *Adv. Polym. Sci.* **1986**, *78*, 115.
(31) Zilg, C.; Mulhaupt, R.; Finter, J. *Macromol. Chem. Phys.* **1999**, *200*, 661.
(32) Chen, J. S.; Poliks, M. D.; Ober, C. K.; Zhang, Y. M.; Wiesner, U.; Giannelis, E. *Polymer* **2002**, *43*, 4895.
(33) Shi, H. Z.; Lan, T.; Pinnavaia, T. J. *Chem. Mater.* **1996**, *8*, 1584.
(34) Franco, M.; Corcuera, M. A.; Gavalda, J.; Valea, A.; Mondragon, I. *J. Polym. Sci., Polym. Phys.* **1997**, *35*, 233.
(35) Triantafillidis, C. S.; LeBaron, P. C.; Pinnavaia, T. J. *Chem. Mater.* **2002**, *14*, 4088.
(36) Ritland, H. N. *J. Am. Ceram. Soc.* **1954**, *37*, 370.
(37) Moynihan, C. T.; Easteal, A. J.; DeBolt, M. A. *J. Am. Ceram. Soc.* **1976**, *59*, 12.
(38) (a) Karasz, F. E.; MacKnight, W. J. *Macromolecules* **1968**, *1*, 537. (b) Shen, M. C.; Eisenberg, A. *Rubber Chem. Technol.* **1970**, *43*, 95.
(39) Cheng, S. Z. D.; Heberer, D. P.; Janimak, J. J.; Lien, S. H.-S.; Harris, F. W. *Polymer* **1991**, *32*, 2053.
(40) (a) Kovacs, A. J. *J. Polym. Sci.* **1958**, *30*, 131. (b) Struik, L. C. E. *Physical Aging in Amorphous Polymers and Other Materials*; Elsevier: Amsterdam, 1978. (c) Struik, L. C. E. *Polymer* **1987**, *28*, 1869. (d) Bartos, J.; Muller, J.; Wendorf, J. H. *Polymer* **1990**, *31*, 1678.
(41) Simon, S. L.; Park, J.-Y.; McKenna, G. B. *Eur. Phys. J. E* **2002**, *8*, 209.
(42) Montserrat, S.; Cortes, P.; Calventus, Y.; Hutchinson, J. M. *J. Polym. Sci., Polym. Phys.* **2000**, *38*, 456.
(43) Hutchinson, J. M.; McCarthy, D.; Montserrat, S.; Cortes, P. *J. Polym. Sci., Polym. Phys.* **1996**, *34*, 229.
(44) Calventus, Y.; Montserrat, S.; Hutchinson, J. M. *Polymer* **2001**, *42*, 7081.
(45) Cortes, P.; Montserrat, S.; Hutchinson, J. M. *J. Appl. Polym. Sci.* **1997**, *63*, 17.
(46) (a) DeBolt, M. A.; Easteal, A. J.; Macedo, P. B.; Moynihan, C. T. *J. Am. Ceram. Soc.* **1976**, *59*, 16. (b) Hodge, I. M.; Huvard, G. S. *Macromolecules* **1983**, *16*, 371. (c) Hodge, I. M. *Macromolecules* **1983**, *16*, 898. (d) Sales, B. C. *J. Non-Cryst. Solids* **1990**, *119*, 136.
(47) (a) Ramos, A. R.; Hutchinson, J. M.; Kovacs, A. J. *J. Polym. Sci., Polym. Phys.* **1984**, *22*, 1655. (b) Hutchinson, J. M.; Ruddy, M. *J. Polym. Sci., Polym. Phys.* **1988**, *26*, 2341. (c) Hutchinson, J. M. *Prog. Colloid Polym. Sci.* **1992**, *87*, 69.
(48) Hutchinson, J. M.; Montserrat, S. *Thermochim. Acta* **2001**, *377*, 63.
(49) Montserrat, S.; Hutchinson, J. M. *Polymer* **2002**, *43*, 351.
(50) Olson, B. G.; Peng, Z. L.; Srithawatpong, R.; McGervey, J. D.; Ishida, H.; Jamieson, A. M.; Manias, E.; Giannelis, E. P. *Mater. Sci. Forum* **1997**, *255*−*257*, 336.
(51) Zax, D. B.; Yang, D. K.; Santos, R. A.; Hegemann, H.; Giannelis, E. P.; Manias, E. *J. Chem. Phys.* **2000**, *112*, 2945.
(52) (a) Tanaka, Y.; Bauer, R. S. In *Epoxy Resins*; May, C. A., Ed.; Marcel Dekker: New York, 1988; p 285. (b) Tanzer, W.; Reinhardt, S.; Fedtke, M. *Polymer* **1993**, *34*, 3520.
(53) Park, J.-Y.; McKenna, G. B. *Phys. Rev. B* **2000**, *61*, 6667.
(54) Loughnane, B. J.; Farrer, R. A.; Scodinu, A.; Fourkas, J. T. *J. Chem. Phys.* **1999**, *111*, 5116.
(55) Fryer, D. S.; Peters, R. D.; Kim, E. J.; Tomaszewski, J. E.; de Pablo, J. J.; Nealey, P. F. *Macromolecules* **2001**, *34*, 5627.
(56) Litvinov, V. M.; Barthel, H.; Weis, J. *Macromolecules* **2002**, *35*, 4356.
(57) (a) Donth, E. *J. Non-Cryst. Solids* **1982**, *53*, 325. (b) Jachson, C. L.; McKenna, G. B. *J. Chem. Phys.* **1990**, *93*, 9002. (c) Fischer, E. W.; Donth, E.; Steffen, W. *Phys. Rev. Lett.* **1992**, *68*, 2344. (d) Hempel, E.; Hempel, G.; Hensel, A.; Schick, C.; Donth, E. *J. Phys. Chem. B* **2000**, *104*, 2460.
(58) Hackett, E.; Manias, E.; Giannelis, E. P. *Chem. Mater.* **2000**, *12*, 2161.
(59) Baschnagel, J.; Binder, K. *J. Phys. I* **1996**, *6*, 1271.
(60) (a) Prucker, O.; Christian, S.; Bock, H.; Rueho, J.; Frank, C. W.; Knoll, W. *Macromol. Chem. Phys.* **1998**, *199*, 1435. (b) Tate, R. S.; Fryer, D. S.; Pasqualini, S.; Montague, M.; de Pablo, J. J.; Nealey, P. F. *J. Chem. Phys.* **2001**, *115*, 9982. (c) Yamamoto, S.; Tsujii, Y.; Fukuda, T. *Macromolecules* **2002**, *35*, 6077.
(61) (a) Fujiwar, S.; Yonezawa, F. *Phys. Rev. Lett.* **1995**, *74*, 4229. (b) Kim, J. S.; Jackman, R. J.; Eisenberg, A. *Macromolecules* **1994**, *27*, 2789. (c) Brosseau, C. *J. Appl. Phys.* **2002**, *91*, 3197. (d) Wu, G. Z.; Asai, S.; Sumita, M. *Macromolecules* **2002**, *35*, 1708.
(62) Feldman, Y.; Kozlovich, N.; Alexandrov, Y. *Phys. Rev. E* **1996**, *54*, 5420.

MA034049B